

High-Pressure Multiphase Behavior of the Ternary Systems (Ethene + Water + Acetone) and (Ethane + Water + Acetone)[†]

Tatiana Ulanova,[‡] Dirk Tuma,[§] and Gerd Maurer*

Department of Mechanical and Process Engineering, University of Kaiserslautern, P.O. Box 3049, D-67653 Kaiserslautern, Germany

The high-pressure phase equilibrium of two ternary systems—(ethene + water + acetone) and (ethane + water + acetone)—was investigated by a static–analytical method. Both systems exhibit the “salting-out” phenomenon upon pressurization by the gaseous compound. The composition of the two coexisting liquid phases L_1 and L_2 of the high-pressure liquid–liquid–vapor (L_1L_2V) equilibrium was determined at (293, 313, and 333) K over the entire pressure range that spans from about (2.9 to 8.0) MPa for (ethene + water + acetone) and from about (2.3 to 5.8) MPa for (ethane + water + acetone), respectively. Additionally, the coordinates of both critical end point lines (i.e., the lower ($(L_1 = L_2)V$) and the upper ($(L_1(L_2 = V))$, respectively) bordering the L_1L_2V equilibrium were recorded between (278 and 353) K. For both systems, it was found that, at constant temperature, increasing the pressure has a stronger impact on the L_2 phase (resulting in higher contents of the gas), whereas the composition of the water-rich L_1 phase is only slightly changed. Furthermore, for both systems, increasing the temperature enlarged the pressure region in which the three-phase L_1L_2V equilibrium is observed, and the corresponding pressures of both critical end point lines were shifted to higher values. In the second part of the work, an approach based on the Peng–Robinson equation of state was employed to model the phase equilibrium data of both ternary systems. Two different mixing rules (that developed by Panagiotopoulos and Reid as well as the mixing rule proposed by Huron and Vidal) were applied. The first procedure resorted to fitting the binary interaction parameters required by the mixing rules to vapor–liquid equilibrium data for the corresponding binary subsystems that were taken from the literature. The calculation results only agreed qualitatively with the experimental data but predicted the main characteristics correctly. In a second procedure, binary interaction parameters were directly fitted to the ternary phase equilibrium data of the experiment instead. A quantitative description of the experimental data could be achieved for both the coordinates of the critical end point lines and the compositions of the coexisting liquid phases L_1 and L_2 at L_1L_2V equilibrium. The maximum mean relative deviations between experimental data and calculation results from that method amount to 19 % for the water mole fraction in the organic phase L_2 of the system (ethene + water + acetone) at 313 K and to 25 % for the gas mole fraction in the aqueous phase L_1 of the system (ethane + water + acetone) at 293 K, respectively. There was no significant difference in the results from the choice of the mixing rule, but a slightly better performance was accomplished by the Panagiotopoulos–Reid mixing rule with a temperature-dependent set of binary interaction parameters.

Introduction

In the present study, the phenomenon of “salting out with a supercritical (or nearcritical) gas” is revisited. In 1959, it was first reported that a binary mixture of water and a water-soluble organic solvent can be forced to split into two liquid phases of different density and composition by pressurization with a super- or nearcritical gas, which means that the operational temperature is in the vicinity of the critical temperature of the gas.¹ The resulting three-phase liquid–liquid–vapor (L_1L_2V) equilibrium exists within a restricted pressure and temperature region. For more than a decade, one of the research focuses of our group has been on the salting-out phenomenon, the corresponding characteristic phase behavior, and its potential for applications in process technology, as, for example, in the field of

liquid–liquid extraction. The phase behavior of several ternary phase-forming systems was investigated in our laboratories. The existence and characteristics of high-pressure phase equilibria were mapped systematically, and the composition data of the coexisting phases (both liquid and vapor) were determined.^{2–6} Parallel to the experimental work, research activity was also comprised to establish an equation-of-state approach to model the experimental results.

The present work continues that research on ternary phase-forming systems with “neutral gases”.^{7,8} In contrast to carbon dioxide as a gaseous compound or salting-out agent, ethene and ethane create a pH-neutral medium upon pressurization, but due to comparable critical data, the general high-pressure phase behavior is rather similar. Moreover, an application which exploits the different hydrophilicity of the coexisting liquid phases to separate thermally or chemically sensitive biocompounds by liquid–liquid extraction in a countercurrent column can profit from pH-neutral phases. Another advantage in those ternary systems is that pH conditions can intentionally be adjusted by the addition of electrolytes.^{9,10}

[†] Part of the “Sir John S. Rowlinson Festschrift”.

* Corresponding author. Tel.: +49 631 205 2410. Fax: +49 631 205 3835. E-mail: gerd.maurer@mv.uni-kl.de.

[‡] Present address: BASF SE, D-67056 Ludwigshafen, Germany.

[§] Present address: BAM Federal Institute for Materials Research and Testing, D-12200 Berlin, Germany.

Before, the two ternary systems (ethene + water + 1-propanol) and (ethene + water + 2-propanol) were investigated at similar operating conditions. Particularly, the compositions of the coexisting phases at high-pressure liquid–liquid–vapor (L_1L_2V) equilibria were determined between (293 and 333) K.

An intention of the present work was to modify the phase-forming compounds in a way that a change is induced in the composition of the coexisting high-pressure liquid phases and particularly in the pressure coordinates of the critical end point lines, while the overall high-pressure phase behavior (of the propanol-containing ternary systems) is maintained. Any application of the three-phase equilibrium would benefit from working at distinctly low pressures as well as from a significant difference in the composition of the coexisting liquid phases L_1 and L_2 . Here, the phase-forming system was modified in such a way that first the alkanol was replaced by the likewise polar compound acetone, and second, ethane became the new gaseous compound. Ethane has a critical temperature that is very close to that of carbon dioxide ($T_c(\text{CO}_2) = 304.1$ K, $T_c(\text{ethane}) = 305.3$ K, $T_c(\text{ethene}) = 282.4$ K).¹¹

Experimental Section

Materials. Ethene (2.7, volume fraction > 0.997) and ethane (2.5, volume fraction > 0.995) were supplied by Messer Griesheim, a subsidiary of the Messer Group GmbH (Krefeld, Germany). Acetone (Uvasol, mass fraction > 0.999 (GC)) was from Merck KGaA (Darmstadt, Germany). Water was deionized and bidistilled before use. Both solvents and gases were used as supplied.

Apparatus, Procedure, and Experimental Uncertainties. The high-pressure apparatus operates according to a static–analytical method and can be employed between about (263 and 353) K and up to a maximum pressure of 30 MPa. The particular arrangement for the present study was exactly the same as that employed for investigating the systems (ethene + water + 1-propanol or 2-propanol).⁷ However, the gas chromatographic procedure applied for the analysis of the coexisting liquid phases was changed. Therefore, that procedure is explained below. Further details are available in Ulanova's doctoral thesis.¹²

In previous work, ethene was charged by means of a membrane compressor. In the present work, (liquid) ethane was supplied either via a diaphragm pump or from a small cylinder by direct condensation into the cell. Prior to the start of the analysis, a period of about 90 min proved sufficient for equilibration in both ternary systems investigated. The gas chromatograph (model HP 5890 series II, Agilent Germany GmbH, Waldbronn, Germany) was equipped with a packed column (Porapak Q, mesh size 80/100, stainless steel, length: 1.5 m, diameter: 1/8 in., Alltech Associates Inc., Deerfield, IL, USA) and a thermal-conductivity detector. Helium was used as the carrier gas, and the software package ChemStation A.09.01 was employed for signal processing and analysis. A new internal sample valve (labeled as V6I–SV in the respective paper by Freitag et al.)⁷ with a smaller volume (of 0.2 μL instead of 1 μL) allowed work without additional heating of the carrier gas line between the sampling valve and the oven. The conditions of the GC analysis were as follows: helium flow rate (both carrier and reference): 25 $\text{mL} \cdot \text{min}^{-1}$; detector temperature: 180 °C; temperature program: initial temperature 50 °C for 0.1 min, temperature increase to the final temperature of 140 °C with a rate of 30 $\text{K} \cdot \text{min}^{-1}$.

The signals (peak areas A_i) from a GC experiment were converted to mole numbers n_i using calibration functions.

$$n_i = \alpha_i A_i \quad (1)$$

The calibration factors α_i were determined by analyzing single-phase ternary mixtures of an exactly known composition that is near to the phase boundary of the L_1L_2V equilibrium region studied. An individual calibration function that proved to be linear was established for each compound of the ternary system and for each sample loop, that is, a total of six calibration functions. The mole fraction x_i is calculated by

$$x_i = \frac{n_i}{\sum_{i=1}^N n_i} \quad (2a)$$

and

$$\sum_{i=1}^N x_i = 1 \quad (2b)$$

The liquids, that is, water and acetone, were added into the cell via the calibrated hand pumps, and the gas came from a small cylinder which was weighed before and after the filling procedure. The volume displacement in a hand pump was calibrated with nitrogen gas at room temperature. All calibration experiments (for (gas + water + acetone)) were performed at 313 K and about 12 MPa, and the calculation of the displaced volume portions of the liquid compounds resorted to density data from the literature (cf., ref 13 for water and ref 14 for acetone, respectively).

The densimeter was calibrated with the pure solvents (i.e., water and acetone, respectively) at the same temperatures as in the analysis of the L_1L_2V equilibrium and over the entire pressure range. The equipment does not allow direct determination of the composition at a critical end point, as any circulation of a critical phase [i.e., either at the lower critical end point, LCEP ($(L_1 = L_2)V$), or at the upper critical end point, UCEP ($(L_1(L_2 = V))$] will instantaneously lead to a phase split. Therefore, only the pressure and temperature coordinates of the critical end points were determined by visual inspection of the content of the view cell. The full procedure is described in two previously published papers.^{7,10}

The temperature was determined with calibrated platinum resistance thermometers. The pressure was determined with pressure transducers that were calibrated in regular intervals during the experiments. For details, the reader is referred to a previous paper⁷ as well as to Ulanova's thesis.¹² The maximum total uncertainty in the temperature measurement was estimated to ± 0.1 K, and the corresponding pressure uncertainty amounted to ± 0.005 MPa for pressures lower than 10 MPa and ± 0.01 MPa for higher pressures, respectively. Visual misconception can result in higher uncertainties (than the intrinsic instrument uncertainties) for the pressure at a critical end point.¹⁰ We estimate that particular uncertainty to ± 0.02 MPa at all pressures.

The estimated experimental uncertainty of the density amounts to ± 2.0 $\text{g} \cdot \text{dm}^{-3}$ at a maximum. That number results from the uncertainty of the literature values for the density of a pure solvent (± 0.5 $\text{g} \cdot \text{dm}^{-3}$) as well as from the uncertainty of the density readings (± 0.03 $\text{g} \cdot \text{dm}^{-3}$).^{7,12}

The uncertainty from the calibration of the gas chromatograph is supposed to have the strongest impact on the corresponding

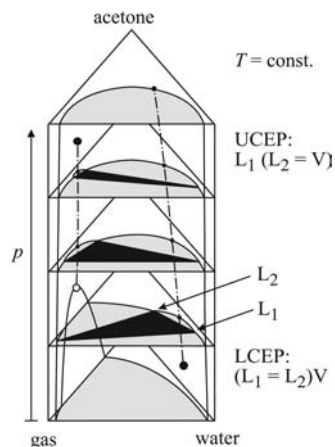


Figure 1. Phase prism that shows the qualitative phase behavior of both ternary phase-forming systems at a temperature T above the critical temperature T_c of the gaseous compound. The shaded area represents two-phase regions (liquid–liquid and vapor–liquid), and the three-phase L_1L_2V equilibrium is indicated in black.

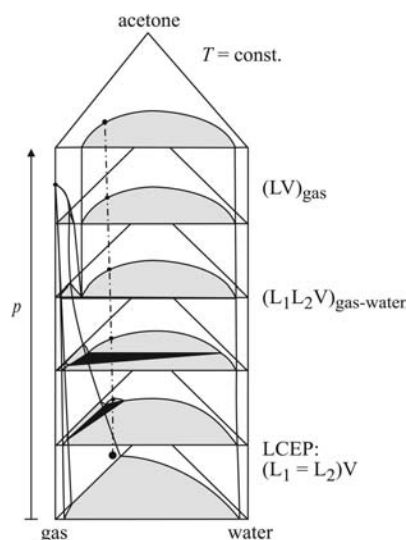


Figure 2. Phase prism that shows the assumed qualitative phase behavior of both ternary phase-forming systems at a temperature T below the critical temperature T_c of the gaseous compound. The shaded area represents two-phase regions (liquid–liquid and vapor–liquid), and the three-phase L_1L_2V equilibrium is indicated in black.

uncertainty of the mole fraction x_i in the coexisting phases. The relative uncertainty of the mole fraction x_i was estimated to be at minimum 1.5 %, ¹² but at very low mole fractions ($x_i < 0.1 \text{ mol} \cdot \text{mol}^{-1}$) it might increase to about 50 %.

Experimental Results and Discussion

In the ternary system (ethene + water + acetone), all investigations to determine the compositions of the coexisting liquid phases L_1 and L_2 of the high-pressure liquid–liquid–vapor (L_1L_2V) equilibrium were performed at temperatures higher than the critical temperature T_c of ethene ($T_c(\text{ethene}) = 282.4 \text{ K}$). ¹¹ The phase behavior at such temperatures is illustrated in Figure 1.

In Figure 1, triangular composition diagrams are arranged to an isothermal phase prism where the pressure increases from bottom to top. The binary subsystems represent the sides of the triangle. The mentioned three-phase L_1L_2V equilibrium of the ternary system is confined by the LCEP line and the UCEP line. At pressures below the LCEP, the binary subsystem (water

Table 1. Experimental Results for the Critical End Point Lines Bordering the Three-Phase L_1L_2V Equilibrium of the System (Ethene + Water + Acetone)

| T/K | p/MPa | |
|-------------------|----------------------|----------------------|
| | LCEP: $(L_1 = L_2)V$ | UCEP: $L_1(L_2 = V)$ |
| 278.15 ± 0.10 | 1.967 ± 0.020 | — |
| 283.15 ± 0.10 | 2.183 ± 0.020 | — |
| 293.15 ± 0.10 | 2.635 ± 0.020 | 5.065 ± 0.020 |
| 303.15 ± 0.10 | 3.135 ± 0.020 | 5.900 ± 0.020 |
| 313.15 ± 0.10 | 3.642 ± 0.020 | 6.965 ± 0.020 |
| 323.15 ± 0.10 | 4.205 ± 0.020 | 7.729 ± 0.020 |
| 333.15 ± 0.10 | 4.640 ± 0.020 | 8.396 ± 0.020 |
| 343.15 ± 0.10 | 5.490 ± 0.020 | 9.226 ± 0.020 |
| 353.15 ± 0.10 | 6.134 ± 0.020 | 10.06 ± 0.02 |

+ acetone) is completely miscible, whereas the two other binary subsystems display a two-phase (liquid–vapor) region. In the region of a three-phase L_1L_2V equilibrium, the composition of the coexisting phases is strongly influenced by the pressure. Ultimately, at pressures above the UCEP, there remains a two-phase equilibrium consisting of a liquid phase and a fluid-like, high-density supercritical gas-rich phase.

At a temperature below the critical temperature of the gaseous compound, the ternary phase-forming system features a different phase behavior. In the present work, such conditions were encountered in the system (ethane + water + acetone) at $T = 293 \text{ K}$. The phase prism at $T < T_c$ is shown in Figure 2.

Increasing the pressure initially results in a very similar phase behavior; however, the three-phase L_1L_2V equilibrium does not end in a UCEP, but in the binary three-phase L_1L_2V equilibrium of the subsystem (gas + water). At even higher pressures, two independent biphasic regions, that is, a liquid–liquid and a liquid–vapor region, exist, and the liquid–vapor region disappears at the vapor pressure of the pure gaseous compound.

The binary subsystems, however, were not subject to experimental investigation in the present work. It is known from the literature that the two binary systems (ethene + water) and (ethane + water) can form hydrates at temperatures below the critical temperature of the pure gas. Already in 1950, a paper on hydrate formation in the system (ethene + water) was published by Diepen and Scheffer. ¹⁵ We also refer to our 2004 paper on the ternary systems (ethene + water + 1-propanol or 2-propanol) which provides a survey of the respective papers including a discussion of the low-temperature phase behavior of the system (ethene + water) published so far. ⁷ Experiments also proved the existence of a metastable binary three-phase L_1L_2V equilibrium in the vicinity of the vapor pressure curve of pure ethene. For the other binary system (ethane + water), a binary three-phase L_1L_2V equilibrium at $T < T_c$ was first

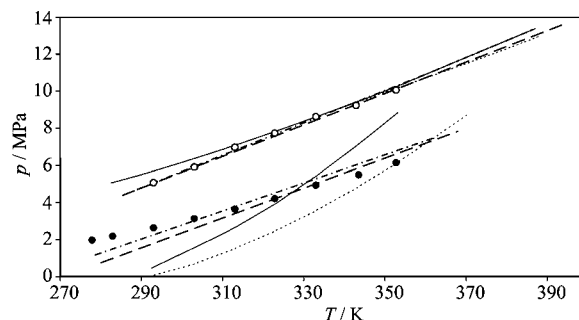


Figure 3. Results for the critical end point lines bordering the three-phase L_1L_2V equilibrium of the system (ethene + water + acetone). Experimental results: ●, LCEP; ○, UCEP. Modeling results, “bin” method: —, PaR mixing rule; ---, HV2 mixing rule. Modeling results, “ter” method: -.-.-, PaR mixing rule; ---, HV2 mixing rule.

Table 2. Experimental Results for the Composition of the Coexisting Phases L₁ and L₂ in the Three-Phase L₁L₂V Equilibrium of the System (Ethene + Water + Acetone)

| p | | $x(\text{ethene})$ | $x(\text{water})$ | $x(\text{acetone})$ | ρ |
|-------------------------|----------------|-----------------------|-----------------------|-----------------------|---------------------|
| MPa | phase | mol·mol ⁻¹ | mol·mol ⁻¹ | mol·mol ⁻¹ | kg·dm ⁻³ |
| $T/K = 293.15 \pm 0.10$ | | | | | |
| 2.863 ± 0.005 | L ₁ | 0.030 ± 0.002 | 0.703 ± 0.011 | 0.267 ± 0.008 | 0.897 ± 0.002 |
| | L ₂ | 0.206 ± 0.006 | 0.233 ± 0.006 | 0.561 ± 0.016 | 0.704 ± 0.002 |
| 3.353 ± 0.005 | L ₁ | 0.020 ± 0.002 | 0.775 ± 0.012 | 0.205 ± 0.006 | 0.924 ± 0.002 |
| | L ₂ | 0.309 ± 0.010 | 0.142 ± 0.004 | 0.549 ± 0.016 | 0.642 ± 0.002 |
| 3.610 ± 0.005 | L ₁ | 0.019 ± 0.002 | 0.792 ± 0.012 | 0.190 ± 0.006 | 0.932 ± 0.002 |
| | L ₂ | 0.347 ± 0.010 | 0.130 ± 0.004 | 0.523 ± 0.016 | 0.596 ± 0.002 |
| 3.900 ± 0.005 | L ₁ | 0.017 ± 0.002 | 0.815 ± 0.012 | 0.168 ± 0.006 | 0.942 ± 0.002 |
| | L ₂ | 0.422 ± 0.012 | 0.083 ± 0.006 | 0.496 ± 0.014 | 0.557 ± 0.002 |
| 4.360 ± 0.005 | L ₁ | 0.015 ± 0.002 | 0.842 ± 0.013 | 0.143 ± 0.004 | 0.949 ± 0.002 |
| | L ₂ | 0.543 ± 0.016 | 0.057 ± 0.004 | 0.401 ± 0.012 | 0.533 ± 0.002 |
| 4.610 ± 0.005 | L ₁ | 0.014 ± 0.002 | 0.857 ± 0.013 | 0.129 ± 0.004 | 0.955 ± 0.002 |
| | L ₂ | 0.638 ± 0.020 | 0.057 ± 0.004 | 0.305 ± 0.010 | 0.522 ± 0.002 |
| 4.970 ± 0.005 | L ₁ | 0.016 ± 0.002 | 0.879 ± 0.013 | 0.105 ± 0.004 | 0.969 ± 0.002 |
| | L ₂ | 0.688 ± 0.020 | 0.042 ± 0.002 | 0.271 ± 0.008 | 0.424 ± 0.002 |
| $T/K = 313.15 \pm 0.10$ | | | | | |
| 3.872 ± 0.005 | L ₁ | 0.034 ± 0.002 | 0.707 ± 0.020 | 0.259 ± 0.008 | 0.876 ± 0.002 |
| | L ₂ | 0.184 ± 0.006 | 0.295 ± 0.006 | 0.521 ± 0.016 | 0.775 ± 0.002 |
| 4.015 ± 0.005 | L ₁ | 0.026 ± 0.002 | 0.746 ± 0.020 | 0.228 ± 0.008 | 0.893 ± 0.002 |
| | L ₂ | 0.214 ± 0.006 | 0.255 ± 0.006 | 0.532 ± 0.016 | 0.763 ± 0.002 |
| 4.410 ± 0.005 | L ₁ | 0.024 ± 0.002 | 0.775 ± 0.020 | 0.201 ± 0.008 | 0.901 ± 0.002 |
| | L ₂ | 0.279 ± 0.008 | 0.193 ± 0.006 | 0.528 ± 0.016 | 0.706 ± 0.002 |
| 4.505 ± 0.005 | L ₁ | 0.020 ± 0.002 | 0.790 ± 0.020 | 0.190 ± 0.008 | 0.904 ± 0.002 |
| | L ₂ | 0.295 ± 0.008 | 0.175 ± 0.006 | 0.531 ± 0.016 | 0.697 ± 0.002 |
| 4.670 ± 0.005 | L ₁ | 0.019 ± 0.002 | 0.800 ± 0.020 | 0.181 ± 0.007 | 0.908 ± 0.002 |
| | L ₂ | 0.325 ± 0.010 | 0.152 ± 0.004 | 0.522 ± 0.016 | 0.688 ± 0.002 |
| 4.780 ± 0.005 | L ₁ | 0.019 ± 0.002 | 0.806 ± 0.020 | 0.175 ± 0.008 | 0.916 ± 0.002 |
| | L ₂ | 0.339 ± 0.010 | 0.148 ± 0.004 | 0.513 ± 0.016 | 0.693 ± 0.002 |
| 4.937 ± 0.005 | L ₁ | 0.019 ± 0.002 | 0.813 ± 0.020 | 0.168 ± 0.008 | 0.920 ± 0.002 |
| | L ₂ | 0.363 ± 0.010 | 0.134 ± 0.004 | 0.502 ± 0.016 | 0.677 ± 0.002 |
| 5.280 ± 0.005 | L ₁ | 0.017 ± 0.002 | 0.832 ± 0.020 | 0.151 ± 0.006 | 0.927 ± 0.002 |
| | L ₂ | 0.424 ± 0.012 | 0.110 ± 0.004 | 0.467 ± 0.014 | 0.646 ± 0.002 |
| 5.475 ± 0.005 | L ₁ | 0.016 ± 0.002 | 0.840 ± 0.020 | 0.144 ± 0.006 | 0.932 ± 0.002 |
| | L ₂ | 0.452 ± 0.012 | 0.103 ± 0.004 | 0.444 ± 0.014 | 0.635 ± 0.002 |
| 5.585 ± 0.005 | L ₁ | 0.015 ± 0.002 | 0.845 ± 0.020 | 0.140 ± 0.006 | 0.935 ± 0.002 |
| | L ₂ | 0.466 ± 0.012 | 0.102 ± 0.004 | 0.431 ± 0.014 | 0.604 ± 0.002 |
| 5.760 ± 0.005 | L ₁ | 0.014 ± 0.002 | 0.851 ± 0.020 | 0.135 ± 0.006 | 0.936 ± 0.002 |
| | L ₂ | 0.501 ± 0.014 | 0.084 ± 0.006 | 0.414 ± 0.014 | 0.552 ± 0.002 |
| 6.080 ± 0.005 | L ₁ | 0.018 ± 0.002 | 0.854 ± 0.020 | 0.128 ± 0.005 | 0.943 ± 0.002 |
| | L ₂ | 0.567 ± 0.015 | 0.086 ± 0.006 | 0.347 ± 0.012 | 0.501 ± 0.002 |
| 6.300 ± 0.005 | L ₁ | 0.022 ± 0.002 | 0.860 ± 0.020 | 0.118 ± 0.005 | 0.945 ± 0.002 |
| | L ₂ | 0.602 ± 0.016 | 0.094 ± 0.006 | 0.304 ± 0.012 | 0.463 ± 0.002 |
| 6.500 ± 0.005 | L ₁ | 0.020 ± 0.002 | 0.870 ± 0.020 | 0.110 ± 0.005 | 0.948 ± 0.002 |
| | L ₂ | 0.656 ± 0.020 | 0.093 ± 0.006 | 0.252 ± 0.012 | 0.449 ± 0.002 |
| 6.650 ± 0.005 | L ₁ | 0.021 ± 0.002 | 0.875 ± 0.020 | 0.105 ± 0.005 | 0.950 ± 0.002 |
| | L ₂ | 0.691 ± 0.020 | 0.090 ± 0.006 | 0.219 ± 0.010 | 0.436 ± 0.002 |
| $T/K = 333.15 \pm 0.10$ | | | | | |
| 5.293 ± 0.005 | L ₁ | 0.028 ± 0.002 | 0.761 ± 0.011 | 0.211 ± 0.004 | 0.882 ± 0.002 |
| | L ₂ | 0.208 ± 0.006 | 0.291 ± 0.008 | 0.501 ± 0.016 | 0.751 ± 0.002 |
| 5.595 ± 0.005 | L ₁ | 0.023 ± 0.002 | 0.789 ± 0.012 | 0.189 ± 0.004 | 0.891 ± 0.002 |
| | L ₂ | 0.239 ± 0.008 | 0.262 ± 0.008 | 0.499 ± 0.014 | 0.719 ± 0.002 |
| 5.880 ± 0.005 | L ₁ | 0.020 ± 0.002 | 0.807 ± 0.012 | 0.173 ± 0.004 | 0.899 ± 0.002 |
| | L ₂ | 0.280 ± 0.008 | 0.214 ± 0.006 | 0.507 ± 0.016 | 0.704 ± 0.002 |
| 6.165 ± 0.005 | L ₁ | 0.020 ± 0.002 | 0.818 ± 0.012 | 0.161 ± 0.004 | 0.911 ± 0.002 |
| | L ₂ | 0.321 ± 0.010 | 0.184 ± 0.006 | 0.495 ± 0.014 | 0.693 ± 0.002 |
| 7.080 ± 0.005 | L ₁ | 0.018 ± 0.002 | 0.847 ± 0.013 | 0.135 ± 0.004 | 0.921 ± 0.002 |
| | L ₂ | 0.431 ± 0.012 | 0.133 ± 0.004 | 0.436 ± 0.014 | 0.626 ± 0.002 |
| 7.730 ± 0.005 | L ₁ | 0.017 ± 0.002 | 0.861 ± 0.013 | 0.122 ± 0.004 | 0.929 ± 0.002 |
| | L ₂ | 0.522 ± 0.014 | 0.112 ± 0.004 | 0.366 ± 0.010 | 0.554 ± 0.002 |
| 8.040 ± 0.005 | L ₁ | 0.022 ± 0.002 | 0.864 ± 0.013 | 0.114 ± 0.004 | 0.932 ± 0.002 |
| | L ₂ | 0.571 ± 0.018 | 0.099 ± 0.003 | 0.329 ± 0.010 | 0.505 ± 0.002 |

observed by Kuenen and Robson in 1899.¹⁶ Later investigations performed at these conditions both demonstrated the formation of hydrates^{17–21} and confirmed the more than 100 year-old observation of a three-phase L₁L₂V equilibrium.²² Moreover, that phase behavior was established as a regular phenomenon in all binary systems (alkane + water) up to *n*-hexane.²²

For more details, for example, regarding exact thermodynamic conditions as well as critical loci and related phe-

nomena illustrated in diagrams, the reader is referred to the review paper by Adrian et al. and the references cited therein.⁶ In the entire present study, the possibility of four-phase equilibria (as discussed in ref 6) was not a subject of particular interest. Notably, the authors of the above-mentioned review paper considered the occurrence of four-phase equilibria in ternary phase-forming systems with acetone as very improbable.

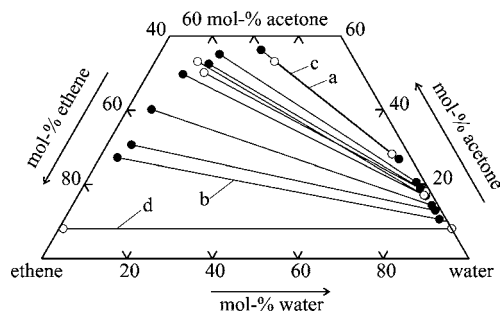


Figure 4. Composition of the coexisting liquid phases L_1 and L_2 of the L_1L_2V equilibrium of (ethene + water + acetone) at $T = 293.15$ K. The tie lines are projected onto a triangular composition diagram; ●, this work, where the corresponding pressures range between (a) 2.863 MPa and (b) 4.970 MPa; ○, data for $T = 288.15$ K from Weinstock's thesis,²³ where the corresponding pressures range between (c) 2.76 MPa (415 psia) and (d) 4.83 MPa (715 psia).

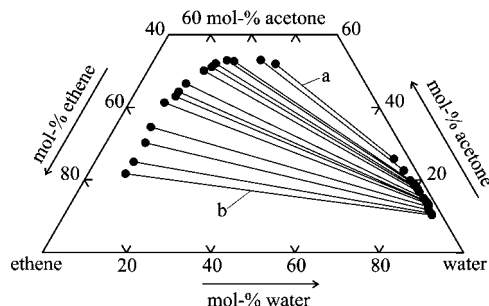


Figure 5. Composition of the coexisting liquid phases L_1 and L_2 of the L_1L_2V equilibrium of (ethene + water + acetone) at $T = 313.15$ K. The tie lines are projected onto a triangular composition diagram, where the corresponding pressures range between (a) 3.872 MPa and (b) 6.650 MPa.

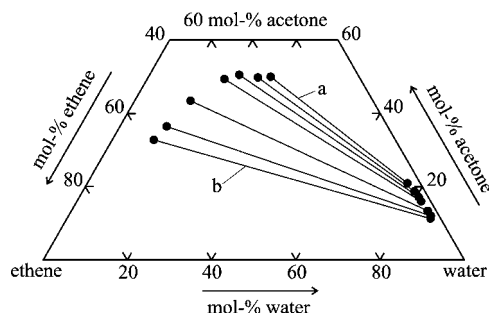


Figure 6. Composition of the coexisting liquid phases L_1 and L_2 of the L_1L_2V equilibrium of (ethene + water + acetone) at $T = 333.15$ K. The tie lines are projected onto a triangular composition diagram, where the corresponding pressures range between (a) 5.293 MPa and (b) 8.040 MPa.

The System (Ethene + Water + Acetone). The experimental results for both critical end point lines of the three-phase L_1L_2V equilibrium are given in Table 1 and shown in Figure 3.

Figure 3 shows that the pressure region of a three-phase L_1L_2V equilibrium at first increases with increasing temperature. Moreover, with further increasing temperature, both critical end point lines merge at the tricritical point, where ($L_1 = L_2 = V$).²⁻⁷ However, the data for the temperature range investigated do not allow for a sound estimation of p, T coordinates at that tricritical point.

The compositions and corresponding densities of the coexisting high-pressure liquid phases L_1 and L_2 are given in Table 2.

Figures 4 to 6 illustrate the phase composition at the three temperatures investigated. The experimental data are shown as projections onto a plane of a triangle composition diagram together with the corresponding tie lines.

Table 3. Experimental Results for the Critical End Point Lines Bordering the Three-Phase L_1L_2V Equilibrium of the System (Ethane + Water + Acetone)

| T/K | p/MPa | |
|---------------|------------------------|----------------------|
| | LCEP: ($L_1 = L_2$)V | UCEP: $L_1(L_2 = V)$ |
| 283.15 ± 0.10 | 1.875 ± 0.020 | — |
| 293.15 ± 0.10 | 2.316 ± 0.020 | — |
| 303.15 ± 0.10 | 2.784 ± 0.020 | — |
| 310.15 ± 0.10 | — | 4.687 ± 0.020 |
| 313.15 ± 0.10 | 3.320 ± 0.020 | 4.875 ± 0.020 |
| 323.15 ± 0.10 | 3.868 ± 0.020 | 5.464 ± 0.020 |
| 333.15 ± 0.10 | 4.440 ± 0.020 | 6.180 ± 0.020 |
| 343.15 ± 0.10 | — | 6.930 ± 0.020 |

At a constant temperature, increasing pressure changes the composition of the phase L_1 toward higher contents of water which is accompanied by a depletion of both ethene and acetone. The coexisting phase L_2 is affected differently, and the pressure effect is more pronounced for L_2 compared to L_1 . There, the ethene content strongly increases, whereas both water and acetone are depleted. Increasing temperatures almost do not have any effect on the phase composition, but the pressure region where a three-phase L_1L_2V equilibrium is observed is broadened (the span between LCEP and UCEP increases from about 2.43 MPa at 293 K to about 3.76 MPa at 333 K), and it is shifted to higher pressures.

The impact of pressure and temperature on the composition of the coexisting liquid phases basically is the same as observed during the investigations of the corresponding ternary systems with 1- or 2-propanol (instead of acetone) being the organic solvent.⁷ The pressure region which borders the three-phase regime is shifted to distinctly higher pressures for both alkanol-containing systems (e.g., at 293.15 K, between [3.998 (7.139) and 16.90 (12.95)] MPa for 1-propanol (2-propanol), and at

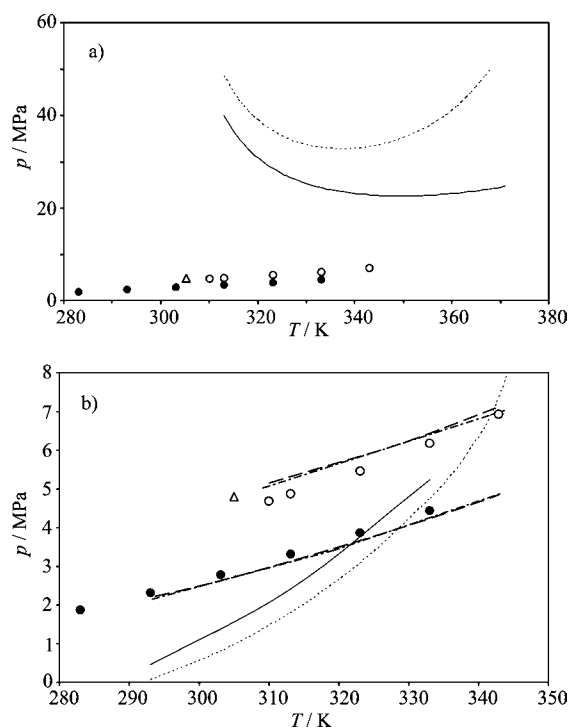


Figure 7. Results for the critical end point lines bordering the three-phase L_1L_2V equilibrium of the system (ethane + water + acetone). Experimental results: ●, LCEP; ○, UCEP; △, critical point of pure ethane.¹¹ Modeling results, "bin" method: —, PaR mixing rule; ---, HV2 mixing rule; (a) shows UCEP lines only. Modeling results, "ter" method: -.-.-, PaR mixing rule; ---, HV2 mixing rule with $wf_{11} = 0.5$.

Table 4. Experimental Results for the Composition of the Coexisting Phases L_1 and L_2 in the Three-Phase L_1L_2V Equilibrium of the System (Ethane + Water + Acetone)

| p MPa | phase | $x(\text{ethane})$ $\text{mol}\cdot\text{mol}^{-1}$ | $x(\text{water})$ $\text{mol}\cdot\text{mol}^{-1}$ | $x(\text{acetone})$ $\text{mol}\cdot\text{mol}^{-1}$ | ρ $\text{kg}\cdot\text{dm}^{-3}$ |
|-------------------------|-------|--|---|---|--|
| $T/K = 293.15 \pm 0.10$ | | | | | |
| 2.332 ± 0.005 | L_1 | 0.028 ± 0.001 | 0.609 ± 0.009 | 0.363 ± 0.010 | 0.861 ± 0.002 |
| | L_2 | 0.167 ± 0.004 | 0.296 ± 0.008 | 0.537 ± 0.016 | 0.757 ± 0.002 |
| 2.429 ± 0.005 | L_1 | 0.017 ± 0.001 | 0.659 ± 0.010 | 0.323 ± 0.010 | 0.880 ± 0.002 |
| | L_2 | 0.224 ± 0.004 | 0.212 ± 0.007 | 0.564 ± 0.016 | 0.727 ± 0.002 |
| 2.500 ± 0.005 | L_1 | 0.012 ± 0.001 | 0.687 ± 0.010 | 0.301 ± 0.010 | 0.891 ± 0.002 |
| | L_2 | 0.264 ± 0.005 | 0.172 ± 0.006 | 0.563 ± 0.016 | 0.702 ± 0.002 |
| 2.571 ± 0.005 | L_1 | 0.009 ± 0.001 | 0.711 ± 0.011 | 0.280 ± 0.008 | 0.898 ± 0.002 |
| | L_2 | 0.347 ± 0.010 | 0.147 ± 0.004 | 0.506 ± 0.016 | 0.675 ± 0.002 |
| 2.686 ± 0.005 | L_1 | 0.004 ± 0.001 | 0.742 ± 0.011 | 0.255 ± 0.008 | 0.903 ± 0.002 |
| | L_2 | 0.418 ± 0.012 | 0.127 ± 0.003 | 0.455 ± 0.014 | 0.656 ± 0.002 |
| 2.750 ± 0.005 | L_1 | 0.002 ± 0.001 | 0.754 ± 0.011 | 0.244 ± 0.008 | 0.907 ± 0.002 |
| | L_2 | 0.475 ± 0.014 | 0.119 ± 0.003 | 0.406 ± 0.012 | 0.634 ± 0.002 |
| $T/K = 313.15 \pm 0.10$ | | | | | |
| 3.530 ± 0.005 | L_1 | 0.018 ± 0.004 | 0.704 ± 0.014 | 0.278 ± 0.006 | 0.875 ± 0.002 |
| | L_2 | 0.260 ± 0.006 | 0.222 ± 0.006 | 0.518 ± 0.010 | 0.713 ± 0.002 |
| 3.710 ± 0.005 | L_1 | 0.014 ± 0.004 | 0.735 ± 0.014 | 0.251 ± 0.006 | 0.889 ± 0.002 |
| | L_2 | 0.340 ± 0.006 | 0.159 ± 0.004 | 0.501 ± 0.010 | 0.681 ± 0.002 |
| 3.867 ± 0.005 | L_1 | 0.009 ± 0.004 | 0.790 ± 0.014 | 0.200 ± 0.008 | 0.903 ± 0.002 |
| | L_2 | 0.417 ± 0.008 | 0.125 ± 0.003 | 0.458 ± 0.009 | 0.660 ± 0.002 |
| 4.047 ± 0.005 | L_1 | 0.012 ± 0.004 | 0.781 ± 0.014 | 0.207 ± 0.006 | 0.908 ± 0.002 |
| | L_2 | 0.519 ± 0.010 | 0.094 ± 0.004 | 0.387 ± 0.008 | 0.639 ± 0.002 |
| 4.177 ± 0.005 | L_1 | 0.007 ± 0.004 | 0.804 ± 0.014 | 0.189 ± 0.005 | 0.919 ± 0.002 |
| | L_2 | 0.595 ± 0.010 | 0.084 ± 0.005 | 0.321 ± 0.007 | 0.614 ± 0.002 |
| 4.306 ± 0.005 | L_1 | 0.014 ± 0.006 | 0.812 ± 0.014 | 0.174 ± 0.005 | 0.922 ± 0.002 |
| | L_2 | 0.647 ± 0.012 | 0.078 ± 0.005 | 0.275 ± 0.006 | 0.557 ± 0.002 |
| 4.477 ± 0.005 | L_1 | 0.007 ± 0.004 | 0.854 ± 0.014 | 0.139 ± 0.004 | 0.935 ± 0.002 |
| | L_2 | 0.684 ± 0.014 | 0.084 ± 0.005 | 0.232 ± 0.006 | 0.490 ± 0.002 |
| 4.727 ± 0.005 | L_1 | 0.006 ± 0.004 | 0.890 ± 0.014 | 0.104 ± 0.003 | 0.953 ± 0.002 |
| | L_2 | 0.704 ± 0.016 | 0.089 ± 0.005 | 0.207 ± 0.006 | 0.334 ± 0.002 |
| $T/K = 333.15 \pm 0.10$ | | | | | |
| 4.512 ± 0.005 | L_1 | 0.029 ± 0.001 | 0.668 ± 0.010 | 0.303 ± 0.005 | 0.831 ± 0.002 |
| | L_2 | 0.165 ± 0.002 | 0.347 ± 0.005 | 0.487 ± 0.007 | 0.736 ± 0.002 |
| 4.712 ± 0.005 | L_1 | 0.015 ± 0.002 | 0.723 ± 0.011 | 0.261 ± 0.004 | 0.861 ± 0.002 |
| | L_2 | 0.235 ± 0.004 | 0.259 ± 0.005 | 0.506 ± 0.008 | 0.713 ± 0.002 |
| 4.917 ± 0.005 | L_1 | 0.008 ± 0.001 | 0.760 ± 0.011 | 0.232 ± 0.003 | 0.876 ± 0.002 |
| | L_2 | 0.296 ± 0.004 | 0.209 ± 0.005 | 0.496 ± 0.007 | 0.682 ± 0.002 |
| 5.079 ± 0.005 | L_1 | 0.005 ± 0.001 | 0.776 ± 0.012 | 0.218 ± 0.003 | 0.883 ± 0.002 |
| | L_2 | 0.336 ± 0.005 | 0.186 ± 0.004 | 0.478 ± 0.007 | 0.670 ± 0.002 |
| 5.350 ± 0.005 | L_1 | 0.003 ± 0.001 | 0.801 ± 0.012 | 0.197 ± 0.003 | 0.896 ± 0.002 |
| | L_2 | 0.414 ± 0.006 | 0.155 ± 0.003 | 0.431 ± 0.006 | 0.605 ± 0.002 |
| 5.482 ± 0.005 | L_1 | 0.001 ± 0.0005 | 0.812 ± 0.012 | 0.187 ± 0.003 | 0.898 ± 0.002 |
| | L_2 | 0.458 ± 0.008 | 0.142 ± 0.004 | 0.400 ± 0.006 | 0.596 ± 0.002 |
| 5.706 ± 0.005 | L_1 | 0.001 ± 0.0005 | 0.828 ± 0.012 | 0.173 ± 0.003 | 0.905 ± 0.002 |
| | L_2 | 0.543 ± 0.008 | 0.119 ± 0.004 | 0.338 ± 0.005 | 0.574 ± 0.002 |
| 5.822 ± 0.005 | L_1 | 0.001 ± 0.0005 | 0.833 ± 0.012 | 0.166 ± 0.004 | 0.910 ± 0.002 |
| | L_2 | 0.599 ± 0.009 | 0.109 ± 0.004 | 0.293 ± 0.005 | 0.574 ± 0.002 |

333.15 K, between [7.878 (12.37) and 20.51 (16.94)] MPa for 1-propanol (2-propanol), respectively). For comparison, the corresponding pressure region for the ternary system (ethane + water + acetone) starts at 2.635 (4.640) MPa and ends at 5.065 (8.396) MPa for 293.15 (333.15) K. Furthermore, the compositions of the coexisting liquid phases differ as well. The phase L_1 in the system (ethane + water + acetone) maintains a lower content of water compared to both propanol-containing systems at all p, T conditions investigated. In phase L_2 , the content of water in the system (ethane + water + acetone) at a pressure near the LCEP is much lower and also more strongly depleted with increasing pressures compared to both systems with 1- or 2-propanol as the organic solvent. Consequently, the concentrations of gas and organic solvent remain significantly higher. For example, at $T = 333.15$ K, at the lowest (highest) pressure investigated for the system (ethane + water + acetone), that is, 5.293 (8.040) MPa, the composition of L_2 is (L_2 is the phase which is much more affected by changing pressures than L_1): $x(\text{ethane}) = 0.208$ (0.571), $x(\text{water}) = 0.291$ (0.099), and $x(\text{acetone}) = 0.501$ (0.329). For the ternary system with

1-propanol (2-propanol) being the organic solvent, the corresponding values for L_2 at $T = 333.15$ K are at minimum pressure $p = 8.568$ (12.62) MPa: $x(\text{ethane}) = 0.079$ (0.118), $x(\text{water}) = 0.666$ (0.618), $x(1\text{-propanol}) = 0.255$, and $x(2\text{-propanol}) = 0.264$, and at maximum pressure $p = 20.10$ (16.62) MPa: $x(\text{ethane}) = 0.502$ (0.409), $x(\text{water}) = 0.207$ (0.281), $x(1\text{-propanol}) = 0.291$, and $x(2\text{-propanol}) = 0.310$.⁷

The pioneering data from Weinstock's thesis at $T = 288.15$ K²³ are the only literature data available and added to Figure 4. Considering the difference of 5 K, those data, which were obtained by a static-analytical apparatus, correspond quite well to our results. The data for L_1 are in a better agreement with our results than the data for L_2 . A stronger discrepancy is observed in the vicinity of the UCEP.

The System (Ethane + Water + Acetone). The experimental results for the second system are presented in the same way as for the previous system. Table 3 and Figure 7 refer to the critical end point lines. As can be seen in Figure 7, the slope of each critical end point line looks exactly the same, but both lines

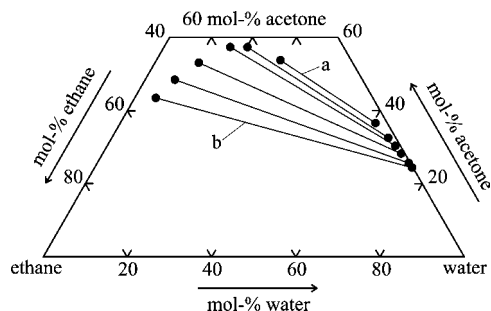


Figure 8. Composition of the coexisting liquid phases L_1 and L_2 of the L_1L_2V equilibrium of (ethane + water + acetone) at $T = 293.15$ K. The tie lines are projected onto a triangular composition diagram, where the corresponding pressures range between (a) 2.332 MPa and (b) 2.750 MPa.

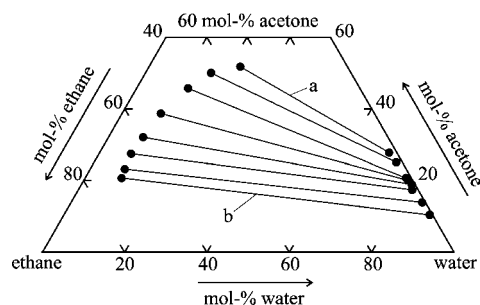


Figure 9. Composition of the coexisting liquid phases L_1 and L_2 of the L_1L_2V equilibrium of (ethane + water + acetone) at $T = 313.15$ K. The tie lines are projected onto a triangular composition diagram, where the corresponding pressures range between (a) 3.530 MPa and (b) 4.727 MPa.

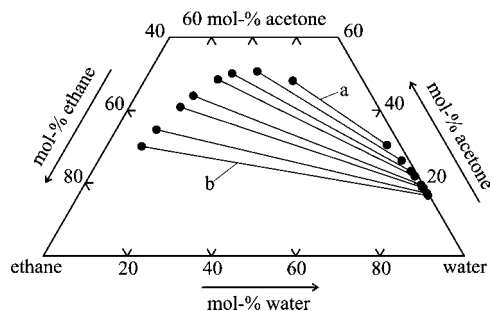


Figure 10. Composition of the coexisting liquid phases L_1 and L_2 of the L_1L_2V equilibrium of (ethane + water + acetone) at $T = 333.15$ K. The tie lines are projected onto a triangular composition diagram, where the corresponding pressures range between (a) 4.512 MPa and (b) 5.822 MPa.

(i.e., the pressure region of the three-phase L_1L_2V equilibrium) are shifted to lower pressures.

The compositions and corresponding densities of the coexisting high-pressure liquid phases L_1 and L_2 are given in Table 4, and the compositions are illustrated in the triangular diagrams of Figures 8 to 10.

The pressure effect on the composition of the coexisting phases L_1 and L_2 at a constant temperature resembles that of the system (ethane + water + acetone). There is a more pronounced depletion of ethane with increasing pressure in the aqueous phase L_1 . The effect of increasing temperature on the phase composition is similar, too. A difference to the system (ethane + water + acetone), however, is the significantly smaller pressure region between LCEP and UCEP (between about 1.56 MPa at 313 K and about 1.74 MPa at 333 K) which is also shifted to lower pressures. Thus, ethane has a stronger salting-out effect. Referring to the previous example, at $T = 333.15$ K,

Table 5. Pure Component Parameters from Melhem et al.²⁴ to Employ in the EoS Model

| component | T_c/K | p_c/MPa | m | n |
|-----------|---------|-----------|--------|--------|
| ethene | 282.4 | 5.04 | 0.4873 | 0.4570 |
| ethane | 305.4 | 4.88 | 0.5336 | 0.2431 |
| water | 647.3 | 22.05 | 0.8893 | 0.0151 |
| acetone | 508.1 | 4.70 | 0.8283 | 0.1495 |

at the lowest (highest) pressure investigated for the system (ethane + water + acetone), that is, 4.512 (5.822) MPa, the composition of L_2 is: $x(\text{ethane}) = 0.165$ (0.599), $x(\text{water}) = 0.347$ (0.109), and $x(\text{acetone}) = 0.487$ (0.293). Consequently, we come to similar conclusions when compared to the propanol-containing systems. Besides, no literature data are available for that system so far.

Modeling Results and Discussion

In previous work, the Peng–Robinson equation of state was used to describe the experimental data of such multicomponent, multiphase systems.⁶ A detailed description of the thermodynamic background, the characteristic workflow, and its performance for typical systems is given in a review paper⁶ as well as in the subsequent 2006 modeling paper on the ternary phase-forming systems (ethane + water + 1- and 2-propanol).⁸ For the sake of brevity, we restrict to listing the main features only.

The Peng–Robinson equation of state (PR-EoS, cf. eq 3) is a typical cubic equation of state.

$$p = \frac{RT}{v-b} - \frac{a(T)}{v(v+b) + b(v-b)} \quad (3)$$

R is the universal gas constant, and v is the molar volume. Parameter a accounts for the attractive interactions. For a pure component, it is given by

$$a(T) = \alpha(T)a(T_c) \quad (4a)$$

$$a(T_c) = 0.45724 \frac{R^2 T_c^2}{p_c} \quad (4b)$$

where p_c and T_c are the critical pressure and the critical temperature, respectively. Parameter b accounts for repulsive interactions. For a pure component it is given by

$$b = 0.07780 \frac{RT_c}{p_c} \quad (5)$$

The model proposed by Melhem et al. is applied to describe the influence of temperature on the parameter a .²⁴

$$\ln \alpha(T) = m(1 - T_r) + n(1 - \sqrt{T_r})^2 \quad \text{where } T_r = T/T_c \quad (6)$$

Consequently, four pure component parameters are required by the model. They are given in Table 5.

The extension from pure compounds to multicomponent mixtures requires mixing rules. In the present study, two mixing rules were employed, the two-parameter, concentration-dependent mixing rule developed by Panagiotopoulos

and Reid (PaR)²⁵ and the likewise two-parameter mixing rule published by Huron and Vidal (HV2).²⁶ The PaR mixing rule is shown in eqs 7a and 7b:

$$a = \sum_{i=1}^{N_C} \sum_{j=1}^{N_C} x_i x_j \sqrt{a_i a_j} (1 - K_{ij}) \quad (7a)$$

$$\text{with } K_{ij} = k_{ij} - (k_{ij} - k_{ji})x_i \quad \text{where } k_{ij} \neq k_{ji} \text{ and } k_{ii} = 0 \quad (7b)$$

A binary mixture, for example, is characterized by two interaction parameters k_{ij} and k_{ji} that might also depend on temperature.

The HV2 mixing rule is a so-called “local-composition” mixing rule, which resorts to the excess Gibbs energy of a mixture and originates from the NRTL model (nonrandom two-liquid) by Renon and Prausnitz.²⁷ The HV2 mixing rule is given in eqs 8a to 11.

$$a = b \sum_{i=1}^{N_C} x_i \left(\frac{a_i}{b_i} - \frac{1}{\Lambda} \frac{\sum_{j=1}^{N_C} x_j C_{ji} b_j \exp\left(-\alpha_{ji} \frac{C_{ji}}{RT}\right)}{\sum_{k=1}^{N_C} x_k b_k \exp\left(-\alpha_{ki} \frac{C_{ki}}{RT}\right)} \right) \quad (8a)$$

$$\text{where } C_{ii} = 0 \quad (8b)$$

$$\text{and } \Lambda \text{ is numerical constant: } \Lambda = \frac{1}{2\sqrt{2}} \ln \left(\frac{2 + \sqrt{2}}{2 - \sqrt{2}} \right) \quad (8c)$$

$C_{ij} (\neq C_{ji})$ is a binary interaction parameter, and $\alpha_{ij} (= \alpha_{ji})$ is a binary volume parameter. With

$$C_{ij} = g_{ij} - g_{ji} \quad (9a)$$

$$\text{with } g_{ij} = \Lambda \frac{a_j}{b_j} \quad (9b)$$

and

$$g_{ij} = -\frac{\sqrt{b_i b_j}}{(b_i + b_j)/2} \sqrt{g_{ii} g_{jj}} (1 - k_{ij}) \quad \text{with} \quad k_{ij} = k_{ji} \text{ and } k_{ii} = 0 \quad (10)$$

For parameter b , a simple mixing rule was employed in all calculations.

$$b = \sum_{i=1}^{N_C} x_i b_i \quad (11)$$

In thermodynamic equilibrium, pressure, temperature, and the fugacity of a compound must be equal in all coexisting phases. The fugacities are calculated from the equation of state. The equal-fugacity condition is commonly solved numerically, for example, employing the Newton–Raphson algorithm. For further details of the mathematical procedure, the reader is referred to the review paper by Adrian et al.⁶

Table 6. Weighting Factors Employed to Fit the Binary Interaction Parameters Using Equation 12

| components | | wf_p | wf_{x_1} | wf_{y_2} |
|------------|---------|--------|------------|------------|
| (1) | (2) | | | |
| ethane | water | 0 | 1 | 1 |
| ethane | acetone | 5 | 0 | 1 |
| ethene | acetone | 5 | 0 | 1 |

Results for the Predictive Model (“bin”). The mixing rules require binary interaction parameters. For the predictive model “bin”, these parameters were determined by correlating vapor–liquid equilibrium data of the binary mixtures. Since the obtained parameters are employed in the model calculation for the ternary systems, this method can be regarded as fully predictive regarding those systems.

The interaction parameters for the binary subsystems [i.e., (ethene + water), (ethane + water), (ethene + acetone), (ethane + acetone), and (water + acetone)] were fitted to—preselected and evaluated—vapor–liquid equilibrium data of the individual systems by minimizing an objective function OF_{bin} , which is the sum of the weighted, squared relative deviations:

$$OF_{\text{bin}} = \sum_{i=1}^{N_D} \left[wf_p \left(\frac{p_{\text{exp}} - p_{\text{calc}}}{p_{\text{exp}}} \right)^2 + wf_{x_1} \left(\frac{x_{1,\text{exp}} - x_{1,\text{calc}}}{x_{1,\text{exp}}} \right)^2 + wf_{y_2} \left(\frac{y_{2,\text{exp}} - y_{2,\text{calc}}}{y_{2,\text{exp}}} \right)^2 \right]_n \quad (12)$$

In eq 12, N_D is the number of input data, and x_1 refers to the mole fraction of (the minor) compound 1 in the liquid phase and y_2 to the mole fraction of (the minor) compound 2 in the vapor phase; wf denotes a weighting factor which considers the different experimental uncertainties of the respective data.

Except for the subsystems (ethene + water) and (ethane + water), T and x_1 were preset, and p and y_2 were calculated. For these two binaries, T and p were preset, because due to the particularly low solubility of ethene (or ethane) in water presetting of T and x_1 would result in a large uncertainty for the calculated pressure p .

Phase equilibrium data for all binary subsystems are available from the open literature, but not equally for each system. Prior to this study, interaction parameters were already determined for the systems (ethene + water)⁸ and (water + acetone),⁶ respectively, according to exactly this method. The weighting factors are given in Table 6, and the literature sources that were resorted to in the procedures of parameter fitting as well as the resulting binary parameters to be finally employed in the model calculation are given in Table 7.

In the following section, the results for the individual binary subsystems are discussed. A comparison between experimental data and calculation results for the vapor–liquid equilibrium of all binary subsystems is provided in Table 8, and auxiliary diagrams which illustrate the results are filed in the Supporting Information (cf. Figures S1 to S6).

Similar to the system (ethene + water),⁸ the high-pressure phase behavior of (ethane + water) is rather complex. The formation of hydrates as well of binary liquid–liquid–vapor equilibria at lower temperatures has already been mentioned. According to the nomenclature developed by van Konynenburg and Scott,³² this binary system shows a type III behavior.³³ Two data sets which cover the p, T region of interest were employed in modeling the system (ethane + water).^{28,29} For the correlation of the vapor–liquid equilib-

Table 7. Binary Interaction Parameters from the Fitting Procedure Using Equation 12

| components | | mixing rule | T/K | p/MPa | N _D , source | k ₁₂ | k ₂₁ or α ₁₂ ^a |
|------------|---------|------------------|---------|------------|-------------------------|-----------------|---|
| (1) | (2) | | | | | | |
| ethene | water | PaR | 308–328 | 0.4–29 | 32, ref 8 | -0.1992 | 0.3511 |
| | | HV2 | 308–328 | 0.4–29 | 32, ref 8 | 0.3560 | 0.1121 |
| ethane | water | PaR | 310–323 | 0.4–65 | 27, refs 28, 29 | -0.1423 | 0.0593 |
| | | PaR ^b | 293 | 0.38–3.6 | 5, ref 28 | -0.1878 | -0.0439 |
| | | PaR ^b | 313 | 0.44–4.7 | 7, ref 28 | -0.1572 | 2.8246 |
| | | PaR ^b | 323 | 0.40–4.8 | 6, ref 28 | -0.1370 | 0.9951 |
| | | PaR ^b | 343 | 0.44–5.0 | 4, ref 28 | -0.1012 | -0.0729 |
| | | HV2 | 274–343 | 0.4–5.0 | 46, ref 28 | 0.7310 | 0.1383 |
| ethene | acetone | PaR | 298–323 | 1.4–7.6 | 18, ref 30 | 0.0758 | 0.0438 |
| | | HV2 | 298–323 | 1.4–7.6 | 18, ref 30 | 0.0366 | -0.0313 |
| ethane | acetone | PaR | 298 | 0.5–4 | 11, ref 31 | 0.1269 | 0.1454 |
| | | HV2 | 298 | 0.5–4 | 11, ref 31 | 0.1521 | 0.0221 |
| water | acetone | PaR | 298–333 | 0.003–0.11 | 72, ref 6 | -0.1279 | -0.2790 |
| | | HV2 | 298–333 | 0.003–0.11 | 72, ref 6 | -0.1455 | 0.2905 |

^a k₂₁ refers to the PaR mixing rule, and α₁₂ to the HV2 mixing rule, respectively. ^b Temperature-dependent binary interaction parameters (instead of a global temperature fit).

Table 8. Comparison between Experimental Data and Calculation Results for the Vapor–Liquid Equilibrium of Binary Systems Employing Binary Interaction Parameters from the Fitting Procedure Using Equation 12^a

| components | | mixing rule | Δx ₁ /x ₁ % | Δp/p/% | Δy ₂ /y ₂ % |
|------------|---------|------------------------|-----------------------------------|------------|-----------------------------------|
| (1) | (2) | | | | |
| ethene | water | PaR | 23, ref 8 | — | 3.8, ref 8 |
| | | HV2 | 5.0, ref 8 | — | 3.6, ref 8 |
| ethane | water | PaR | 12 | — | — |
| | | PaR, ^b 293K | 0.5 | — | — |
| | | PaR, ^b 313K | 2.1 | — | — |
| | | PaR, ^b 323K | 1.0 | — | — |
| | | PaR, ^b 343K | 1.5 | — | — |
| | | HV2 | 3.2 | — | — |
| ethene | acetone | PaR | — | 3.4 | 9.6 |
| | | HV2 | — | 4.0 | 9.5 |
| ethane | acetone | PaR | — | 1.7 | 4.7 |
| | | HV2 | — | 1.4 | 3.6 |
| water | acetone | PaR | — | 6.1, ref 6 | 3.1, ref 6 |
| | | HV2 | — | 4.8, ref 6 | 2.7, ref 6 |

^a Pressure *p*, temperature *T*, and number of data *N_D* are given in Table 7. ^b Temperature-dependent binary interaction parameters (instead of a global temperature fit).

$$\frac{\Delta X}{X} = \frac{1}{N_D} \sum_{n=1}^{N_D} \left| \frac{X_{\text{exp}} - X_{\text{calc}}}{X_{\text{exp}}} \right|_n \text{ with } X = p, x_1, y_2$$

rium, the PaR mixing rule wrongly results in an increasing solubility of ethane in water with increasing temperature, when the interaction parameters are temperature-independent. Introduction of a temperature dependency, however, reproduces the correct solubility behavior. Notably, the interaction parameter *k*₂₁ has a minor influence on the calculation results compared to *k*₁₂. *k*₂₁ can even be set zero, and no significant change is observed. The average relative deviation between experimental and modeled solubility data (mole fraction of ethane in water) amounts to 12 % for temperature-independent parameters. The introduction of temperature-dependent parameters, however, reduces that number significantly to 2.1 % at 313 K and 0.5 % at 293 K, respectively. The HV2 mixing rule improves the results significantly and gives the correct temperature behavior. The average relative deviation between experimental and modeled solubility data (mole fraction of ethane in water) amounts to 3.2 %.

The vapor–liquid data of the system (ethane + acetone) are rather limited, and we generated the interaction parameters employing data from one particular study.³⁰ Both mixing rules

give quite similar results. For example, the mean relative deviation between experimental and calculated data using the PaR (HV2) mixing rule (for preset numbers of temperature and liquid phase composition) amounts to 3.4 % (4.0 %) for the pressure and 9.6 % (9.5 %) for the mole fraction of acetone in the vapor phase, respectively. Experimental data and model calculations show simple type I behavior according to the classification by van Konynenburg and Scott.

For the system (ethane + acetone), parameter fitting resorted to the data published by Ohgaki et al. at a single temperature (298 K).³¹ As for the previous system, both mixing rules perform similarly. The corresponding deviation values using the PaR (HV2) mixing rule are 1.7 % (1.4 %) for the pressure and 4.7 % (3.6 %) for the mole fraction of acetone in the vapor phase, respectively. The equation-of-state calculation shows a three-phase L₁L₂V equilibrium at low temperatures (e.g., at (293 and 313) K) with a bordering vapor–liquid and liquid–liquid equilibrium with a strong evidence for type III.

Results of the “bin” Model for the Ternary Systems. It was shown in the previous study on the propanol-containing ternary systems⁸ that the “bin” method of the EoS model predicts the existence of a three-phase L₁L₂V equilibrium, but there is only a qualitative agreement with experimental data. The same statement holds for the two systems investigated here. A comprehensive comparison between experimental data and calculation results for the composition of the coexisting high-pressure liquid phases L₁ and L₂ is given in Table 9.

Figure 3 shows the experimental data and the calculation results for the critical end point lines of the system (ethane + water + acetone). Both mixing rules correctly reproduce the trend, and the reproduction of the UCEP line (L₁(L₂ = V) above about 310 K comes off well. For the UCEP line, even at temperatures below 300 K, the mean relative deviation Δ*p*/*p* does not surmount 12 %. Regarding the composition of the coexisting liquid phases, Figure 11 exemplarily shows a triangle diagram with both experimental and calculation results at *p* = 5.9 MPa and *T* = 333 K for both mixing rules. A look at Table 9 demonstrates that for the aqueous phase L₁ agreement is best for the mole fraction of water (i.e., the main compound) and worst for the mole fraction of ethane (i.e., the minor compound). The corresponding result for the organic phase L₂ is more diffuse. The worst agreement is mostly found for water, whereas the best agreement is alternately found for ethene or for acetone. Figure 11 also shows the (calculated) composition of the vapor

Table 9. Comparison between Experimental Data and Calculation Results for the Coexisting Liquid Phases L₁ and L₂ of the Three-Phase L₁L₂V Equilibrium for Constant Temperatures and over the Entire Data^a

| components | | | mixing rule | method, T of processed data set | L ₁ | | | L ₂ | | |
|------------|-------|---------|-------------|---------------------------------|---------------------|---------------------|---------------------|---------------------|---------------------|---------------------|
| (1) | (2) | (3) | | | $\Delta x_1/x_1/\%$ | $\Delta x_2/x_2/\%$ | $\Delta x_3/x_3/\%$ | $\Delta x_1/x_1/\%$ | $\Delta x_2/x_2/\%$ | $\Delta x_3/x_3/\%$ |
| ethene | water | acetone | PaR | bin, 293 K | 62 | 7.2 | 25 | 9.0 | 56 | 12 |
| | | | | bin, 313 K | 23 | 4.4 | 19 | 9.4 | 207 | 7.8 |
| | | | | bin, 333 K | 58 | 29 | 46 | 23 | 76 | 4.6 |
| | | | | ter, all data | 63 | 11 | 45 | 10 | 24 | 8 |
| | | | | ter*, 293 K | 15 | 2.7 | 8.4 | 6.5 | 11 | 5.6 |
| | | | | ter*, 313 K | 15 | 1.0 | 4.3 | 7.1 | 19 | 8.3 |
| | | | | ter*, 333 K | 9.3 | 0.7 | 3.5 | 5.5 | 9.1 | 3.8 |
| | | | HV2 | bin, 293 K | 65 | 5.2 | 13 | 6.1 | 58 | 13 |
| | | | | bin, 313 K | 150 | 1.7 | 9.1 | 8.5 | 233 | 10 |
| | | | | bin, 333 K | 43 | 4.3 | 30 | 13 | 33 | 13 |
| | | | | ter, all data | 21 | 3.2 | 11 | 4.8 | 13 | 3.5 |
| | | | | bin, 293 K | 71 | 19 | 39 | 33 | 31 | 22 |
| | | | | bin, 313 K | 71 | 5.8 | 30 | 57 | 133 | 65 |
| | | | | bin, 333 K | > 1000 | 11 | 31 | 49 | 103 | 18 |
| ethane | water | acetone | PaR | bin*, 293 K | 50 | 18 | 44 | 34 | 35 | 15 |
| | | | | bin*, 313 K | 49 | 5.9 | 37 | 33 | 79 | 11 |
| | | | | bin*, 333 K ^b | 760 | 11 | 26 | 46 | 84 | 9.1 |
| | | | | ter, all data | 46 | 6.9 | 23 | 17 | 15 | 15 |
| | | | | ter*, 293 K | 25 | 3.8 | 9.1 | 7.9 | 9.6 | 5.4 |
| | | | | ter*, 313 K | 19 | 3.3 | 13 | 16 | 20 | 18 |
| | | | | ter*, 333 K | 19 | 5.2 | 18 | 1.9 | 7.8 | 2.8 |
| | | | HV2 | bin, 293 K | 77 | 14 | 28 | 56 | 29 | 35 |
| | | | | bin, 313 K | 30 | 6.3 | 35 | 74 | 123 | 94 |
| | | | | bin, 333 K | > 1000 | 20 | 74 | 85 | 181 | 35 |
| | | | | ter, all data, $wf_{11} = 0.1$ | 73 | 2.5 | 7.4 | 7.1 | 13.5 | 7.3 |
| | | | | ter, all data, $wf_{11} = 0.5$ | 67 | 3.0 | 12 | 7.5 | 15 | 8.1 |

^a “bin” = binary interaction parameters from a fit to binary data (over all temperatures), “bin*” denotes temperature-dependence of k_{12} and k_{21} (cf. Table 7), “ter” = binary interaction parameters from a fit to ternary data (over all temperatures), “ter*” = temperature-dependent interaction parameters (cf. Table 10). ^b With k_{12} and k_{21} from binary fit to data for $T = 343$ K (cf. Table 7).

$$\frac{\Delta X}{X} = \frac{1}{N_D} \sum_{n=1}^{N_D} \left| \frac{(X_{\text{exp}} - X_{\text{calc}})}{X_{\text{exp}}} \right|_n \text{ with } X = (x_1, x_2, x_3)_{L_1, L_2}$$

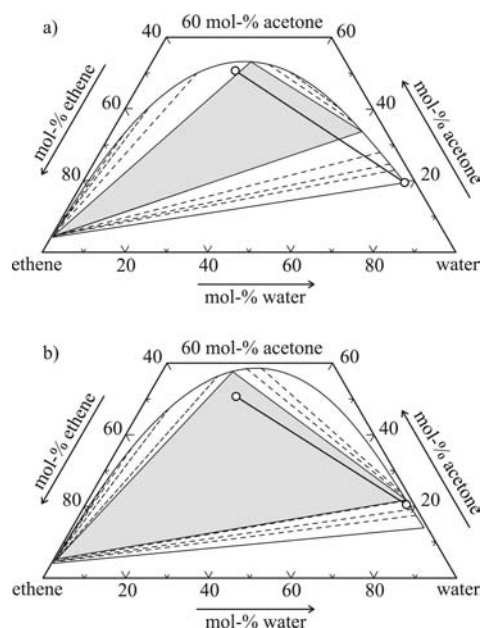


Figure 11. Three-phase L₁L₂V equilibrium of (ethene + water + acetone) at $p = 5.9$ MPa and $T = 333.15$ K. Comparison between experimental data for L₁ and L₂ (O) and calculation results from the “bin” method. (a) PaR mixing rule; (b) HV2 mixing rule.

phase V, but no evaluation is possible due to the lack of experimental data. In that example, the PaR mixing rule produces a higher discrepancy for the composition of L₁, whereas the composition of L₂ is reproduced by both mixing rules in a similar quality. From an overall view, however, there

is no significant difference between the employed mixing rules. The individual biases of the results compensate each other.

Switching to the system (ethane + water + acetone) deteriorated the modeling results significantly. As shown in Figure 7, the modeling results for the UCEP line L₁(L₂ = V) for both mixing rules are far off the experiment and of an unrealistic shape. The corresponding pressure discrepancy amounts up to about 1 order of magnitude, whereas the results for the LCEP line are similar to the results for the ethene-containing system. A test with temperature-dependent binary interaction parameters k_{12} and k_{21} in the PaR mixing rule improved the modeling results of the vapor–liquid data of the binary subsystem (ethane + water). Figure 12 shows the compositions of L₁ and L₂ at $p = 5.4$ MPa and $T = 333$ K. All three sets of mixing rules perform in a similar way for the ternary system (ethane + water + acetone) and also show the same deviation behavior for the individual concentrations like that for the previously discussed ternary system. Although the introduction of temperature-dependent parameters k_{12} and k_{21} in the PaR mixing rule improved modeling the binary subsystem (ethane + water) (cf. Table 8), no distinctive improvement is observed for the ternary system.

Results for the Correlation Model (“ter”). In contrast to the predictive model “bin”, the binary interaction parameters were determined by correlating the actual experimental data of the ternary system. Of course, the genuinely predictive character of the model is lost, but in addition to the data correlation, a certain ability to predict the phase behavior in adjacent p, T regions can be expected. Furthermore, that method may be regarded as a test whether a selected

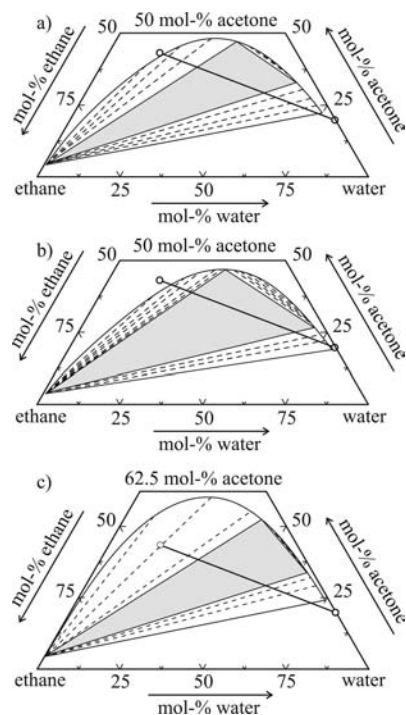


Figure 12. Three-phase L_1L_2V equilibrium of (ethane + water + acetone) at $p = 5.4$ MPa and $T = 333.15$ K. Comparison between experimental data for L_1 and L_2 (○) and calculation results from the “bin” method. (a) PaR mixing rule, interaction parameters independent of temperature; (b) PaR mixing rule, interaction parameters dependent on temperature; (c) HV2 mixing rule.

combination of equation of state and mixing rules is appropriate at all.

In the “ter” model, the interaction parameters for the binary subsystems were directly fitted to the compositions of the coexisting liquid phases of the ternary mixture. The corresponding objective function OF_{ter} is:

$$OF_{\text{ter}} = \sum_{n=1}^{N_D} \left[\sum_{j=1}^{N_p} \left[\sum_{i=1}^{N_C} \left(w_{fij} \left(\frac{x_{i,\text{exp}} - x_{i,\text{calc}}}{x_{i,\text{exp}}} \right)^2 \right) \right] \right]_n$$

where $N_C = N_p = 3$ (13)

N_C , N_p , and w_{fij} are the number of compounds, the number of phases, and weighting factors, respectively. All weighting factors were set to one ($w_{fij} = 1$). The resulting binary interaction parameters are given in Table 10.

Results of the “ter” Model for the Ternary Systems. The correlation method results in smaller discrepancies to the corresponding experimental data than the prediction method (cf. Table 9).

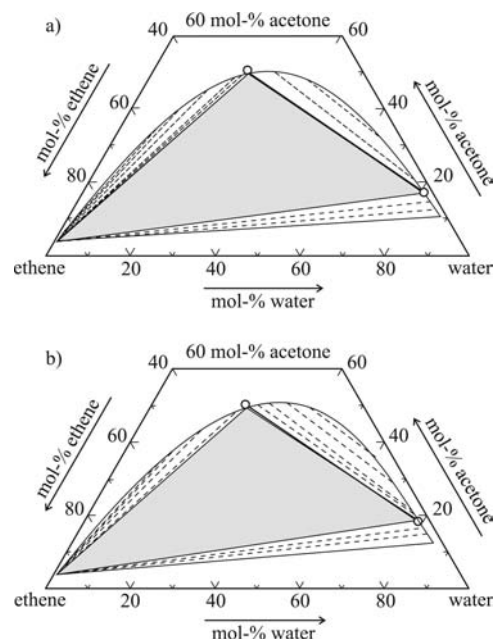


Figure 13. Three-phase L_1L_2V equilibrium of (ethene + water + acetone) at $p = 5.9$ MPa and $T = 333.15$ K. Comparison between experimental data for L_1 and L_2 (○) and calculation results from the “ter” method. (a) PaR mixing rule, interaction parameters dependent on temperature; (b) HV2 mixing rule.

The critical end point lines of the system (ethene + water + acetone) are already shown in Figure 3.

Both mixing rules reproduced the phase borderlines well, and the diagram also shows that a prediction toward higher temperatures, particularly for the UCEP, is possible. The results for modeling the composition of L_1 and L_2 of that system at $p = 5.9$ MPa and $T = 333$ K are shown in Figure 13.

Table 9 shows that both the “ter” and the “bin” method give identical results regarding the question for which individual compound the coincidence is best or worst. The results for the phase L_2 are better than for the phase L_1 . Surprisingly, the HV2 mixing rule created better results than the PaR mixing rule without temperature-dependent interaction parameters, but the PaR mixing rule with temperature-dependent interaction parameters performed almost equally.

Like with the “bin” method, the system (ethane + water + acetone) shows larger discrepancies. The critical end point lines, which are shown in Figure 7, could still be reproduced within a mean relative deviation for the pressure $\Delta p/p$ of about 6 % by using both mixing rules. Since the solubility of ethane in the aqueous phase L_1 is particularly low, several weighting factors $w_{f11} \neq 1$ were tested. Better results were obtained using $w_{f11} = 0.5$, further reduction did no longer show a significant

Table 10. Binary Interaction Parameters from the Fitting Procedure Using Equation 13

| components | | | mixing rule | k_{12} | k_{21} | α_{12} | k_{13} | k_{31} | α_{13} | k_{23} | k_{32} | α_{23} |
|----------------------|---------|------------|----------------------|----------|------------|---------------|----------|------------|---------------|----------|------------|---------------|
| (1) | (2) | (3) | | | | | | | | | | |
| ethene | water | acetone | PaR | -0.2050 | 0.3340 | — | 0.0408 | 0.0489 | — | -0.1331 | -0.2582 | — |
| | | | PaR, 293 K | -0.2647 | 0.2001 | — | 0.0835 | 0.0484 | — | -0.1290 | -0.2832 | — |
| | | | PaR, 313 K | -0.1996 | 0.0744 | — | 0.0129 | 0.0392 | — | -0.1394 | -0.2823 | — |
| | | | PaR, 333 K | -0.1859 | 0.0813 | — | 0.0778 | 0.0501 | — | -0.1018 | -0.2652 | — |
| | | | HV2 | -0.7250 | $= k_{12}$ | 0.0658 | 0.0649 | $= k_{13}$ | 0.0050 | -0.1437 | $= k_{23}$ | 0.3071 |
| ethane | water | acetone | PaR | 0.2685 | -0.3200 | — | 0.0689 | 0.0977 | — | -0.2361 | -0.2633 | — |
| | | | PaR, 293 K | 0.0718 | -0.0054 | — | 0.0378 | 0.0642 | — | -0.2290 | -0.2675 | — |
| | | | PaR, 313 K | -0.0635 | 0.1219 | — | -0.2122 | 0.0156 | — | -0.2991 | -0.3026 | — |
| | | | PaR, 333 K | 0.1466 | -0.0184 | — | 0.0337 | 0.0723 | — | -0.2167 | -0.2506 | — |
| | | | HV2, $w_{f11} = 0.1$ | -0.2734 | $= k_{12}$ | -0.1309 | 0.1049 | $= k_{13}$ | 0.0124 | -0.1984 | $= k_{23}$ | 0.2174 |
| HV2, $w_{f11} = 0.5$ | -0.3039 | $= k_{12}$ | -0.1658 | 0.1005 | $= k_{13}$ | 0.0080 | -0.2065 | $= k_{23}$ | 0.1913 | | | |

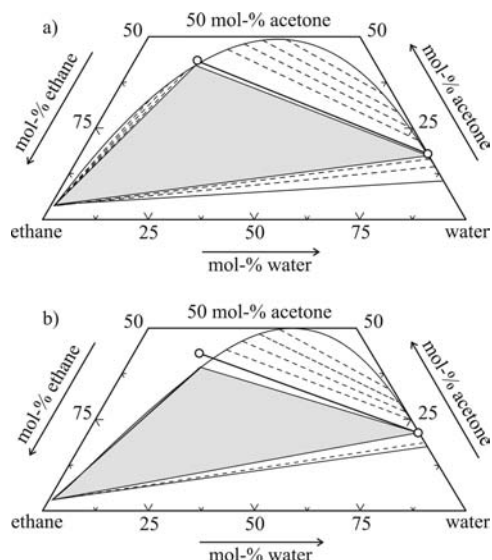


Figure 14. Three-phase L_1L_2V equilibrium of (ethane + water + acetone) at $p = 5.4$ MPa and $T = 333.15$ K. Comparison between experimental data for L_1 and L_2 (O) and calculation results from the “ter” method. (a) PaR mixing rule, interaction parameters dependent on temperature; (b) HV2 mixing rule with $wf_{11} = 0.5$.

improvement. The results for the correlation of the phase composition are exemplarily shown in Figure 14 for $p = 5.4$ MPa and $T = 333$ K.

Table 9 and Figure 14 demonstrate that the system (ethane + water + acetone) shows the same qualitative pattern as the system (ethene + water + acetone). Similarly, the introduction of a temperature-dependent binary interaction parameter in the PaR mixing rule improved the correlation. For example, the mean relative deviation for the mole fractions in L_1 was reduced by a factor of about two, but the effect on the corresponding values for L_2 , however, was not that pronounced. The HV2 mixing rule provides results of comparable quality already with temperature-independent interaction parameters, except for the mole fraction of ethane in the phase L_1 .

Conclusions

The existence of a noticeable pressure-induced three-phase L_1L_2V equilibrium at near-critical temperatures of a ternary system (gas + water + hydrophilic organic solvent) may be employed in extraction and separation techniques, particularly in the field of biotechnology, if certain requirements are fulfilled by the system. First, the phase split should be triggered at low pressures (preferably < 10 MPa), and the pressure-range of the three-phase region should be rather large. Additionally, the compositions of the coexisting liquid phases L_1 and L_2 should both differ significantly (separation capability) from each other and be sensitive to pressure changes (tunability). Second, a more complex phase behavior, such as the occurrence of another three-phase equilibrium or even a four-phase $L_1L_2L_3V$ equilibrium at operating conditions, should be avoided, as it might seriously affect the feasibility of such applications.

The two ternary systems investigated in the present study (at temperatures between (278 and 353) K) match all of those criteria. The p,T coordinates of the phase borderlines and the compositions and densities of the coexisting liquid phases were experimentally determined and additionally modeled by an approach based on the Peng–Robinson equation of state.

The basic idea was to investigate a ternary system that is pH-neutral. Therefore, the previously used gas carbon dioxide

was replaced by ethene and alternatively ethane. Furthermore, the previously used alkanols (1- and 2-propanol) were replaced by the more polar organic compound acetone. The coexisting liquid phases L_1 and L_2 of both ternary systems have compositions that are rather similar for both systems. The distinguishing feature is the pressure. Ethane displays a slightly more pronounced salting-out effect. For example, at 293 K, the liquid–liquid phase split occurs at 2.3 MPa (with ethane), whereas a pressure of nearly 2.6 MPa is required for ethene.

The modeling results proved that the selected equation-of-state approach is always able to at least qualitatively predict the existence of such a three-phase L_1L_2V equilibrium. However (and as expected from previous investigations), the quality of the calculations depends on the experimental data used to determine binary interaction parameters. A fully predictive approach (where all binary interaction parameters were determined from vapor–liquid equilibrium data of the binary subsystems) describes the phase behavior of the systems qualitatively but unfortunately results in large uncertainties for the phase compositions and p,T coordinates of the phase borderlines. When all binary interaction parameters were adjusted exclusively to phase equilibrium data of the ternary mixture, the approach gives a good agreement between calculated and experimental data. However, in that case the equation of state gives only a poor agreement with experimental data for the vapor–liquid equilibrium of the binary subsystems.

Supporting Information Available:

Diagrams showing the vapor–liquid equilibrium behavior of the binary subsystems (ethane + water), (ethene + acetone), and (ethane + acetone). This material is available free of charge via the Internet at <http://pubs.acs.org>.

Literature Cited

- Elgin, J. C.; Weinstock, J. J. Phase equilibrium at elevated pressures in ternary systems of ethylene and water with organic liquids. Salting out with a supercritical gas. *J. Chem. Eng. Data* **1959**, *4*, 3–12.
- Wendland, M.; Hasse, H.; Maurer, G. Multiphase high-pressure equilibria of carbon dioxide–water–isopropanol. *J. Supercrit. Fluids* **1993**, *6*, 211–222.
- Wendland, M.; Hasse, H.; Maurer, G. Multiphase high-pressure equilibria of carbon dioxide–water–acetone. *J. Supercrit. Fluids* **1994**, *7*, 245–250.
- Adrian, T.; Hasse, H.; Maurer, G. Multiphase high-pressure equilibria of carbon dioxide–water–propionic acid and carbon dioxide–water–isopropanol. *J. Supercrit. Fluids* **1996**, *9*, 19–25.
- Adrian, T.; Oprea, S.; Maurer, G. Experimental investigation of the multiphase high-pressure equilibria of carbon dioxide–water–(1-propanol). *Fluid Phase Equilib.* **1997**, *132*, 187–203.
- Adrian, T.; Wendland, M.; Hasse, H.; Maurer, G. High-pressure multiphase behaviour of ternary systems carbon dioxide–water–polar solvent: review and modeling with the Peng–Robinson equation of state. *J. Supercrit. Fluids* **1998**, *12*, 185–221.
- Freitag, J.; Sanz Diez, M. T.; Tuma, D.; Ulanova, T. V.; Maurer, G. High-pressure multiphase behavior of the ternary systems (ethene + water + 1-propanol) and (ethene + water + 2-propanol). Part I: Experimental investigation. *J. Supercrit. Fluids* **2004**, *32*, 1–13.
- Freitag, J.; Tuma, D.; Ulanova, T. V.; Maurer, G. High-pressure multiphase behavior of the ternary systems (ethene + water + 1-propanol) and (ethene + water + 2-propanol). Part II: Modeling. *J. Supercrit. Fluids* **2006**, *39*, 174–186.
- Adrian, T.; Freitag, J.; Maurer, G. A novel high-pressure liquid–liquid extraction process for downstream processing in biotechnology: extraction of cardiac glycosides. *Biotechnol. Bioeng.* **2000**, *69*, 559–565.
- Ulanova, T.; Tuma, D.; Maurer, G. Salt effect on the high-pressure multiphase behavior of the ternary system (ethene + water + 2-propanol). *J. Chem. Eng. Data* **2009**, *54*, 1417–1420.
- Wagner, W.; Overhoff, U. *ThermoFluids Version 1.0 (Build 1.0.0)*; Springer Verlag: Berlin, 2006.
- Ulanova, T. Untersuchungen zum Einsatz von Hochdruck-Mehrphasengleichgewichten mit überkritischen Gasen zur Abtrennung von

- Naturstoffen aus wässrigen Lösungen. Doctoral thesis (Doctor of Engineering), University of Kaiserslautern, Germany, 2007.
- (13) Jones, F. E.; Harris, G. L. IST-90 density of water formulation for volumetric standards calibration. *J. Res. Natl. Inst. Stand. Technol.* **1992**, *97*, 335–340.
 - (14) Riddick, J. A.; Bunger, W. B.; Sakano, T. K. *Organic Solvents, Physical Properties and Methods of Purification*; John Wiley & Sons: New York, 1986.
 - (15) Diepen, G. A. M.; Scheffer, F. E. C. The ethene-water system. *Recl. Trav. Chim.* **1950**, *69*, 593–603.
 - (16) Kuenen, J. P.; Robson, W. G. On the mutual solubility of liquids.—vapour-pressure and critical points. *Philos. Mag. Ser. 5* **1899**, *48*, 180–203.
 - (17) Roberts, O. L.; Brownscombe, E. R.; Howe, L. S. Constitution diagrams and composition of methane and ethane hydrates. *Oil Gas J.* **1940**, *39*, 37–40.
 - (18) Holder, G. D.; Grigoriou, G. C. Hydrate dissociation pressures of (methane + ethane + water). Existence of a locus of minimum pressures. *J. Chem. Thermodyn.* **1980**, *12*, 1093–1104.
 - (19) Holder, G. D.; Hand, J. H. Multi-phase equilibria in hydrates from methane, ethane, propane and water mixtures. *AIChE J.* **1982**, *28*, 440–447.
 - (20) Danneil, A.; Tödheide, K.; Franck, E. U. Verdampfungsgleichgewichte und kritische Kurven in den Systemen Äthan/Wasser und n-Butan/Wasser bei hohen Drücken. *Chem. Ing. Tech.* **1967**, *39*, 816–822.
 - (21) Chapoy, A.; Coquelet, C.; Richon, D. Measurement of the water solubility in the gas phase of the ethane + water binary system near hydrate forming conditions. *J. Chem. Eng. Data* **2003**, *48*, 957–966.
 - (22) Mokraoui, S.; Coquelet, C.; Valtz, A.; Hegel, P. E.; Richon, D. New solubility data of hydrocarbons in water and modeling concerning vapor-liquid-liquid binary systems. *Ind. Eng. Chem. Res.* **2007**, *46*, 9257–9262.
 - (23) Weinstock, J. J. Phase equilibrium at elevated pressures in ternary systems of ethylene and water with organic liquids. Ph.D. Thesis, Princeton University: Princeton, NJ, 1954.
 - (24) Melhem, G. A.; Saini, R.; Goodwin, B. M. A modified Peng-Robinson equation of state. *Fluid Phase Equilib.* **1989**, *47*, 189–237.
 - (25) Panagiotopoulos, A. Z.; Reid, R. C. New mixing rule for cubic equations of state for highly polar, asymmetric systems. In *Equations of State—Theories and Applications*; Chao, K. C., Robinson, R. L., Eds.; ACS Symposium Series: Washington, DC, 1986; Vol. 300, pp 571–582.
 - (26) Huron, M. J.; Vidal, J. New mixing rules in simple equations of state for representing vapour-liquid equilibria of strongly non-ideal mixtures. *Fluid Phase Equilib.* **1979**, *3*, 255–271.
 - (27) Renon, H.; Prausnitz, J. M. Local compositions in thermodynamic excess functions for liquid mixtures. *AIChE J.* **1968**, *14*, 135–144.
 - (28) Mohammadi, A. H.; Chapoy, A.; Tohidi, B.; Richon, D. Measurements and thermodynamic modelling of vapor-liquid equilibria in ethane-water systems from 274.26 to 343.08 K. *Ind. Eng. Chem. Res.* **2004**, *43*, 5418–5424.
 - (29) Culberson, O. L.; McKetta, J. J., Jr. Phase equilibria in hydrocarbon-water systems. II - The solubility of ethane in water at pressures to 10,000 psi. *Petr. Trans. Am. Inst. Mining Met. Eng.* **1950**, *189*, 319–322.
 - (30) Yokoyama, C.; Masuoka, H.; Arai, K.; Saito, S. Vapor-liquid equilibria for the methane-acetone and ethylene-acetone systems at 25 and 50 °C. *J. Chem. Eng. Data* **1985**, *30*, 177–179.
 - (31) Ohgaki, K.; Sano, F.; Katayama, T. Isothermal vapor-liquid equilibrium data for binary systems containing ethane at high pressures. *J. Chem. Eng. Data* **1976**, *21*, 55–58.
 - (32) van Konynenburg, P. H.; Scott, R. L. Critical lines and phase equilibria in binary van der Waals mixtures. *Philos. Trans. R. Soc. London, Ser. A* **1980**, *298*, 495–540.
 - (33) Aparicio-Martínez, S.; Hall, K. R. Phase equilibria in water containing binary systems from molecular based equations of state. *Fluid Phase Equilib.* **2007**, *254*, 112–125.

Received for review June 1, 2010. Accepted August 13, 2010.

JE100609R